

Probing low-energy QCD with kaonic atoms at DAΦNE

M Tüchler¹, J Zmeskal¹, A Amirkhani², C Amsler¹, A Baniahmad², M Bazzi³, D Bosnar⁴, M A Bragadireanu⁵, P Bühler¹, M Cargnelli¹, M Carminati², A Clozza³, C Curceanu³, R Del Grande^{3,9}, L De Paolis³, L Fabbietti⁶, C Fiorini², C Guaraldo³, M Iliescu³, M Iwasaki⁷, P Levi Sandri³, J Marton^{1,3}, M Miliucci³, P Moskal⁸, S Niedzwiecki⁸, S Okada⁷, K Piscicchia^{3,9}, A Scordo³, M Silarski⁸, D Sirghi^{3,5}, F Sirghi^{3,5}, M Skurzok^{3,8}, A Spallone³, O Vazquez Doce^{3,6} and E Widmann¹

¹ Stefan-Meyer-Institute, Boltzmanngasse 3, 1090 Vienna, Austria

² Politecnico Milano and INFN Sezione di Milano, Milano, Italy

³ INFN, Laboratori Nazionali di Frascati, Frascati (Roma), Italy

⁴ Department of Physics, Faculty of Science, University of Zagreb, Zagreb, Croatia

⁵ Horia Hulubei National Inst. of Physics and Nuclear Engineering, Bucharest, Romania

⁶ Excellence Cluster Universe, Technische Universität München, Garching, Germany

⁷ RIKEN Nishina Center, RIKEN, Wako, 351-0198, Japan

⁸ M. Smoluchowski Institute of Physics, Jagiellonian University, Krakow, Poland

⁹ Museo Storico della Fisica e Centro Studi e Ricerche "Enrico Fermi", Roma, Italy

E-mail: marlene.tuechler@oeaw.ac.at, johann.zmeskal@oeaw.ac.at

Abstract. X-ray spectroscopy of kaonic atoms provides a versatile tool to study the strong interaction at low energies via a direct observation of its influence on the ground state of kaonic hydrogen atoms. The SIDDHARTA experiment provided precise results on the energy shift and width of the kaonic hydrogen $1s$ state induced by the strong interaction. To enable the extraction of the antikaon-nucleon scattering lengths a_0 and a_1 , SIDDHARTA-2 aims to determine the energy shift and width in kaonic deuterium with precisions of 30 eV and 75 eV, respectively. This measurement is aggravated by the low kaonic deuterium X-ray yield and a high background environment and will only be possible by implementing a severe upgrade on the SIDDHARTA apparatus.

1. Introduction

The low-energy, non-perturbative regime of quantum chromodynamics (QCD) still leaves important questions unanswered, e.g. the generation of the hadron masses. To contribute to these open questions, the antikaon-nucleon interaction is of particular interest as a testing ground for chiral SU(3) symmetry in QCD and for the role of explicit chiral symmetry breaking due to the relatively large strange quark mass. Kaonic hydrogen atoms [1] offer the ideal framework to study strong-interaction processes including strangeness at threshold, which will give access to the basic low-energy parameters, like the antikaon-nucleon scattering lengths.

Now, the K^-p reaction is well understood from the recent results of kaonic hydrogen



measurements obtained from KpX [2] at KEK, DEAR at DAΦNE [3] and finally from SIDDHARTA (Silicon Drift Detectors for Hadronic Atom Research by Timing Application) at DAΦNE [4], along with theoretical calculations based on these results ([5], [6]). One has to consider that the theoretical approaches are complicated due to the presence of the $\Lambda(1405)$ resonance located just below the K^-p threshold. At present, there are no lattice QCD calculations of antikaon-nucleon scattering lengths, although a theoretical framework has been proposed [6]. Even though the importance of antikaon deuterium atom X-ray spectroscopy has been well recognized for more than 30 years [7], no experimental results have yet been obtained due to the difficulty of the X-ray measurement.

2. The Antikaon Source - DAΦNE

In order to perform the antikaonic deuterium measurement, a negatively charged kaon beam is necessary. With DAΦNE, a world-class electron-positron collider at the Laboratori Nazionali di Frascati (LNF) in Italy is available to produce low-momentum antikaons. The DAΦNE accelerator complex consists of an e^+e^- Linac, a damping ring used for both beams and a twin rings collider, which was originally planned for two interaction regions [8]. After a luminosity upgrade only one interaction region is available. The total energy of the beams in the reference system of the centre of the mass is equal to 1.02 GeV, corresponding to the mass of the Φ meson. The cross section for this process is $\sim 5 \mu\text{b}$. About 50% of the almost at rest produced Φ mesons will decay into a K^+K^- pair producing a monochromatic “kaon beam” with a momentum of about 127 MeV/c, with a momentum spread $\Delta p/p < 0.1\%$.

3. Formation of Kaonic Hydrogen

When a negatively charged kaon enters a target, it is slowed down to a kinetic energy of a few tens of eV by ionizations and excitations of the target molecules. Finally, it will be captured into an outer atomic orbit by replacing an electron and thus forming a kaonic atom. The initial principal quantum number n of the exotic atom is given by the reduced mass μ and the electron mass m_e with the principal quantum number n_e of the outermost electron shell:

$$n \approx \sqrt{\frac{\mu}{m_e}} n_e \quad (1)$$

For kaonic hydrogen, the kaon starts from an outer shell with a main quantum number $n \sim 25$ to cascade down to the $1s$ ground state. Especially for kaonic hydrogen atoms, the Stark effect will become important during the cascade process, mixing the states with the same principal quantum number. For kaonic atoms, this means that the nuclear kaon absorption may occur even from higher n -orbits with low l -states. Therefore, Stark mixing is, besides the kaon decay, mainly responsible for a drastic reduction of the X-ray yield with increasing target density. For gaseous hydrogen with about 1.5% of liquid hydrogen density only 1% of the captured kaons will reach the $1s$ ground state.

4. The SIDDHARTA Kaonic Hydrogen Results

The SIDDHARTA experiment at LNF [4] at DAΦNE aimed to determine the kaonic hydrogen $1s$ shift and width with high precision. The development of a cryogenic gaseous target cell, surrounded by specially developed large area Silicon Drift Detectors (SDDs) are cornerstones of the SIDDHARTA setup. These large area SDD chips were developed within a European research project (HadronPhysics3) [9]. Their operating temperature of about 170 K allows to achieve an energy resolution of 160 eV (FWHM) at 6 keV. The timing resolution (given by the drift time of the electrons in the active detector) was below 1 μsec . Overall 48 SDDs, each with 3 cm^2 active area and a thickness of 450 μm , were placed around the target cell.

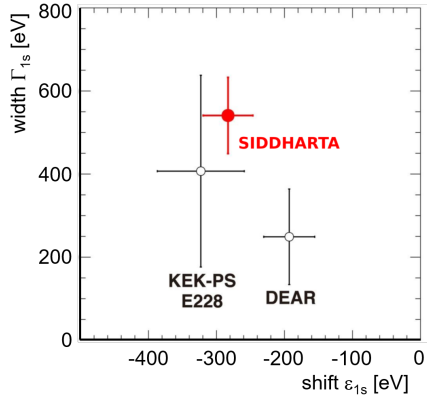


Figure 1. Comparison of experimental results for shift and width of the kaonic hydrogen 1s state; KEK-PS [2], DEAR [3] and SIDDHARTA [4].

The most precise values of the strong interaction induced shift and width of the kaonic hydrogen 1s state were obtained by the SIDDHARTA experiment:

$$\begin{aligned}\epsilon_{1s} &= -283 \pm 36_{stat} \pm 6_{syst} \text{ eV} \\ \Gamma_{1s} &= 541 \pm 89_{stat} \pm 22_{syst} \text{ eV}.\end{aligned}$$

The results of the pioneering KpX experiment (KEK-PS E228), the DEAR experiment, and the SIDDHARTA experiment are shown in figure 1.

The SIDDHARTA result (red datapoint in figure 2) helped to significantly reduce the theoretical uncertainties of the scattering amplitude at the K^-N threshold ([5],[6]) and the K^-p scattering length a_{K^-p} is given with inclusion of Coulomb corrections [5]:

$$\begin{aligned}\text{Re } a_{K^-p} &= (-0.65 \pm 0.10) \text{ fm} \\ \text{Im } a_{K^-p} &= (0.81 \pm 0.15) \text{ fm}.\end{aligned}$$

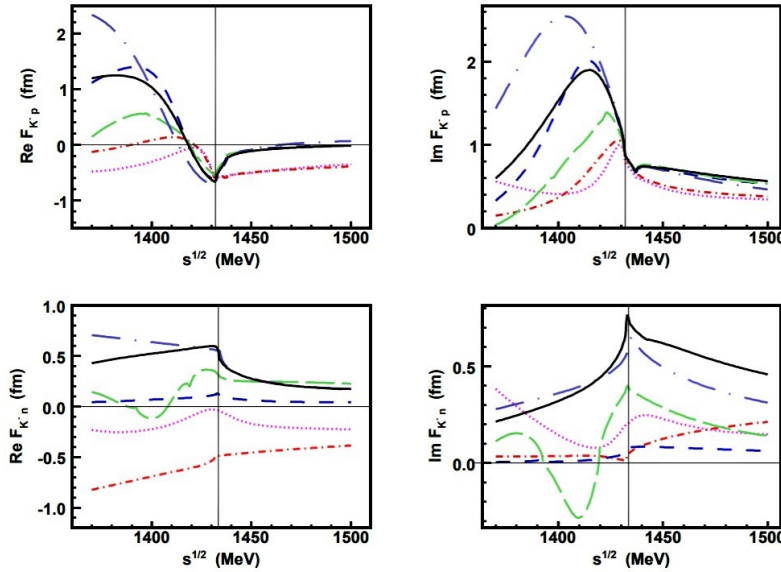


Figure 2. Energy dependence of the elastic K^-p (top) and K^-n (bottom) forward scattering amplitude extrapolated to the subthreshold region, generated with different models: Prague (dot-long-dashed), Kyoto-Munich (continuous), Murcia1 (dashed), Murcia2 (long-dashed), Bonn4 (dot-dashed) and Bonn2 (dotted) (*Graph taken from [10]*).

Additionally, below threshold there is still a large discrepancy, which strongly depends on the used models (figure 2). For K^-p the Kyoto-Munich (continuous) and Murcia1 (dashed) models are in reasonable agreement. For K^-n the Kyoto-Munich and Prague (dot-long-dashed) models agree quite well, while the other models deviate not only in terms of the amplitude but also in the qualitative shape of the energy dependence. Further experimental input is necessary and will become available by a K^-d measurement, which allows to extract the K^-n scattering length, further constraining theoretical calculations.

5. The Quest for Kaonic Deuterium

The experimentally determined values for shift and width of kaonic hydrogen are related to the s-wave scattering lengths at threshold. Due to isospin conservation only the average value of the isospin $I = 0$ and $I = 1$ scattering lengths (a_0 and a_1) can be obtained from a kaonic hydrogen measurement. The s-wave complex scattering lengths a_{K^-p} and a_{K^-d} are related to the isoscalar and isovector scattering lengths a_0 and a_1 through the simplified expressions

$$a_{K^-p} = \frac{1}{2}(a_0 + a_1), \quad a_{K^-d} \sim \frac{1}{2}(a_{K^-p} + a_{K^-n}) \sim \frac{1}{4}(a_0 + 3a_1), \quad a_{K^-n} = a_1. \quad (2)$$

Therefore, the kaonic deuterium measurement is crucial to disentangle a_0 and a_1 .

On the theoretical side, there are many recent publications predicting quite inconsistent values for shift and width of the kaonic deuterium $1s$ state (see table 1), which have to be further constrained by experimental data.

Table 1. Theoretical calculations of the expected values for the energy shift ϵ_{1s} and width Γ_{1s} of the ground state in kaonic deuterium.

ϵ_{1s} (eV)	Γ_{1s} (eV)	Reference
-670	1016	Weise <i>et al.</i> (2017) [11]
-887	757	Mizutani <i>et al.</i> (2013) [12]
-787	1011	Shevchenko (2012) [13]
-779	650	Meißner <i>et al.</i> (2011) [6]
-769	674	Gal (2007) [14]
-884	665	Meißner <i>et al.</i> (2011) [15]
-1080	1024	Oset (2001) [16]

6. The Experimental Method to Measure K^-d

The proposed kaonic deuterium experiment SIDDHARTA-2 at DAΦNE will measure the transition X-ray energies to the ground state of kaonic deuterium atoms (a similar experiment is planned at J-PARC, E57). The experimental challenges of kaonic deuterium measurements are the very low kaonic deuterium X-ray yield, the even larger ground state width compared to kaonic hydrogen and the difficulty to perform X-ray spectroscopy in the radiation environment of DAΦNE. Therefore, it is crucial to develop a large area X-ray detector system to optimise on the signal side and to control and increase the signal-to-background ratio by improving the timing performance as well as to implement charge particle veto systems. Three main updates are important for the new instrumental apparatus:

- Development of a new monolithic Silicon Drift Detector (SDD) array with the goal to produce SDD-chips to withstand high background rates, with good energy resolution (~ 150 eV) and a drift time below 500 ns. In addition, the active-to-total area has to be drastically improved, allowing for an efficient coverage of the X-ray detectors around the target cell.
- Design and construction of a lightweight cryogenic gaseous target system.
- Design and implementation of a charged particle veto system to suppress beam related background events. For SIDDHARTA-2, inner and outer veto detector systems have been developed.

6.1. The Silicon Drift Detectors

New SDD arrays were developed at FBK together with Milano Politecnico, LNF-INFN and SMI for SIDDHARTA-2 ([17], [18] [19]). In total, 48 SDD arrays will be arranged around the target cell. One SDD array consists of eight single SDD units, each with an active area of 8×8 mm². Due to the layout of the SDD arrays and a special support structure, the dead area of the total detector system could be minimised. A significant improvement compared to the previously used SDDs is the change of the preamplifier system with the implementation of a CMOS preamplifier

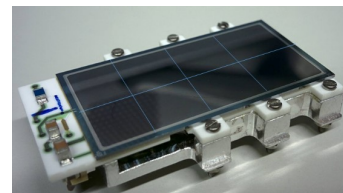


Figure 3. Array of eight SDD units on the ceramic structure.

(CUBE) mounted on the ceramic carrier directly connected to the anode. As a result, the SDDs are almost independent of the applied bias voltages and temperature fluctuations, and operate with increased stability.

6.2. The Lightweight Cryogenic Target Cell

The cylindrical target cell with a height of 130 mm and a diameter of 144 mm (see figure 4) is a lightweight construction with the lateral wall made of polyamide foils (Kapton) with a thickness of $\sim 150 \mu\text{m}$, allowing for a transmission of 90% for 8 keV X-rays. The target cell is operated at cryogenic temperatures to achieve a sufficiently high density at relatively low working pressure, i.e. 3% LDD at 0.3 MPa for 30 K.

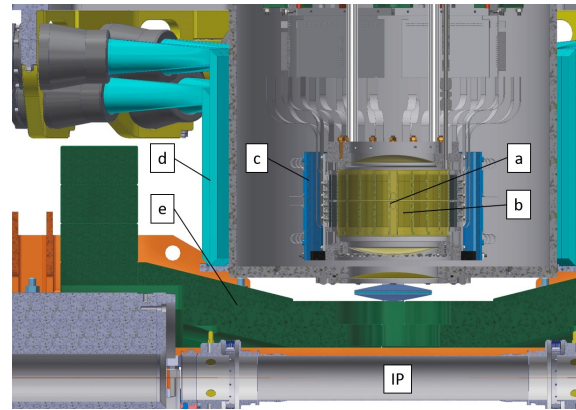


Figure 4. Cryogenic target cell (a) surrounded by the SDDs (b) and Veto-2 counters (c). Outside of the vacuum chamber, the Veto-1 detectors (d) and lead shielding (e) are mounted. The interaction point is marked with IP.

6.3. The Veto Detection Systems

The two-stage veto system contributes to the increase of the signal-to-background ratio by a factor of three. Its outer part, called the Veto-1, consists of twelve units of scintillators with photomultiplier (PMT) read-out and is located outside of the vacuum chamber [20].

The Veto-1 is mainly dedicated to using timing information to distinguish between kaon stops in the target gas and kaon stops in the entrance window or target sidewall. In both cases, charged pions are produced. For the kaon stopping in the gas, the kaonic atom formation and cascade process - and hence the pion emission - take much longer than in a solid. For this distinction, a time resolution of $\sim 500 \text{ ps}$ is required. Therefore, a sophisticated detector design is needed (figure 4). To achieve a time resolution independent of the particle hit position, the scintillator is read out on both ends with PMTs despite the limited space around the vacuum chamber. A mirror connects the scintillators to light guides on the back side. On both ends, light collectors lead to the PMTs.

Directly surrounding the SDDs, the inner part of the veto system, the Veto-2 [21], is mounted (figure 4), responsible for the suppression of a signal-correlated background component in the form of minimum ionizing particles (MIPs). This form of background (mainly protons and pions) results from the absorption of the kaon on the nucleons and hence cannot be eliminated by the use of timing information. Instead, the spatial correlation between events in the SDDs and in the Veto-2 counters in coincidence with the kaon trigger is determined. Depending on the path of the MIPs through the SDDs, signals mimicking X-rays in the region of interest (ROI) might be produced. MIPs passing the SDDs on the edge of their active area or passing the ceramic structure, producing delta rays, or backscattered electrons from the surrounding setup can produce these events. The Veto-2 is comprised of 24 units of four detectors. Each of the 96 detectors consists of a $50 \times 12 \times 4 \text{ mm}^3$ plastic scintillator with silicon photomultiplier (SiPM) read-out on one side with a mean time resolution of $(293 \pm 45) \text{ ps}$ and a detection efficiency of over 99% [21].

6.4. Dedicated Monte Carlo Simulation

For SIDDHARTA-2, dedicated Monte Carlo (MC) studies were performed showing that the newly designed apparatus will allow to perform the K^-d experi-

ment, with following main assumptions: shift $\epsilon_{1s} = -800$ eV, width $\Gamma_{1s} = 800$ eV and X-ray yield = 0.1% (a factor of ten less than for kaonic hydrogen).

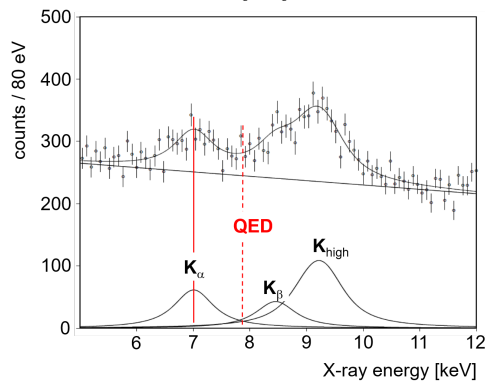


Figure 5. Simulated energy spectrum with the peak of the $2p \rightarrow 1s$ K_α transition and the position of the purely electromagnetic $2p \rightarrow 1s$ QED transition are indicated.

provide the most important experimental information missing in the field of the low-energy antikaon-nucleon interaction today.

Additionally, the dedicated lead shielding structure and veto devices were included in the MC simulations for SIDDHARTA-2, leading to a signal-to-background ratio of 1:4. By fitting these produced spectra (figure 5), the precision of shift and width was evaluated to be 30 eV and 75 eV, respectively, for an integrated luminosity of 800 pb^{-1} , comparable to the SIDDHARTA K^-p results.

7. Summary

The most precise values of the ground state shift and width of kaonic hydrogen, measured by SIDDHARTA, have to be extended to a first measurement of kaonic deuterium to extract the isospin dependent isoscalar a_0 and isovector a_1 $\bar{K}N$ scattering lengths. The kaonic deuterium X-ray measurement performed by SIDDHARTA-2 will

Acknowledgments

Part of this work was supported by the Austrian Science Fund (FWF), Doctoral program No. W1252-N27; the Grant-in-Aid for Specially Promoted Research (20002003), MEXT, Japan; Croatian Science Foundation under Project IP-2018-01-8570; Ministero degli Affari Esteri e della Cooperazione Internazionale, Direzione Generale per la Promozione del Sistema Paese (MAECI), StrangeMatter project; Polish National Science Center through grant No. UMO-2016/21/D/ST2/01155; Ministry of Science and Higher Education of Poland grant no 7150/E-338/M/2018.

References

- [1] Curceanu C *et al.* 2019 *Rev. Mod. Phys.* **91** 025006
- [2] Iwasaki M *et al.* 1997 *Phys. Rev. Lett.* **78** 3067
- [3] Beer G *et al.* 2005 *Phys. Rev. Lett.* **94** 212302
- [4] Bazzi M *et al.* 2011 *Phys. Lett. B* **704** 113
- [5] Ikeda Y, Hyodo T and Weise W 2011 *Phys. Lett. B* **706** 63
- [6] Döring M and Meißner U-G 2011 *Phys. Lett. B* **704** 663
- [7] Dalitz *et al.* 1982 *Proc. Int. Conf. Hypernuclear and Kaon Physics* ed Povh B (Heidelberg) p 201
- [8] Vignola G *et al.* 1996 *Frascati Phys. Ser.* **4** 19
- [9] Bazzi M *et al.* 2011 *Nucl. Instrum. Methods Phys. A* **628** 264
- [10] Cieplý A, Mai M, Meißner U-G and Smejkal J 2016 *Nucl. Phys. A* **954** 17
- [11] Hoshino T *et al.* 2017 *Phys. Rev. C* **96** 045204
- [12] Mizutani T, Fayard C, Saghai B and Tsushima K 2013 *Phys. Rev. C* **87** 035201
- [13] Shevchenko N V 2015 *Phys. Lett. B* **744** 105
- [14] Gal A 2007 *Int. J. Mod. Phys. A* **22** 226
- [15] Meißner U-G, Raha U and Rusetzky A 2006 *Eur. Phys. J. C* **47** 473
- [16] Kamakov S S, Oset E, Ramos A 2001 *Nucl. Phys. A* **690** 494
- [17] Quaglia R *et al.* 2015 *IEEE T. Nucl. Sc.* **62(1)** 221-227
- [18] Schembari F *et al.* 2016 *IEEE T. Nucl. Sc.* **63(3)** 1797-1807
- [19] Tripl C *et al.* 2018 *J. Phys.: Conf. Series* **1138** 012013
- [20] Bazzi M *et al.* 2013 *J. Instrum.* **8** T11003
- [21] Tüchler M *et al.* 2018 *J. Phys.: Conf. Series* **1138** 012012